One- and two-mode squeezed light in correlated interferometry

One- and two-mode squeezed light in correlated interferometry

I. Ruo-Berchera,[1] I. P. Degiovanni,[1] S. Olivares,[2,3] N. Samantaray,[1,4] P. Traina,[1] and M. Genovese[1,5]
[1]*INRIM, Strada delle Cacce 91, I-10135 Torino, Italy*
[2]*Dipartimento di Fisica, Università degli Studi di Milano, Via Celoria 16, I-20133 Milano, Italy*
[3]*Istituto Nazionale di Fisica Nucleare, Sezione di Milano, Via Celoria 16, I-20133 Milano, Italy*
[4]*Politecnico di Torino, Corso Duca degli Abruzzi 24, I-10129 Torino, Italy*
[5]*Istituto Nazionale di Fisica Nucleare, Sezione di Torino, Via P. Giuria 1, I-10125 Torino, Italy*
(Received 6 July 2015; published 9 November 2015)

We study in detail a system of two interferometers aimed at detecting extremely faint phase fluctuations. This system can represent a breakthrough for detecting a faint correlated signal that would remain otherwise undetectable even using the most sensitive individual interferometric devices, as in the case of so-called holographic noise. The signature of this kind of noise emerges as a correlation between the output signals of the interferometers. On the other hand, when holographic noise is absent one expects uncorrelated signals since the time-averaged fluctuations due to shot noise and other independent contributions vanish (though limiting the overall sensitivity). We show how injecting quantum light in the free ports of the interferometers can reduce the photon noise of the system beyond the shot noise, enhancing the resolution in the phase-correlation estimation. We analyze the use of both the two-mode squeezed vacuum and two independent squeezed states. Our results confirm the benefit of using squeezed beams together with strong coherent beams in interferometry. We also investigate the possible use of the two-mode squeezed vacuum, discovering interesting and unexplored areas of application of bipartite entanglement, in particular the possibility of reaching in principle a surprising uncertainty reduction.

DOI: 10.1103/PhysRevA.92.053821 PACS number(s): 42.50.St, 42.25.Hz, 03.65.Ud, 04.60.−m

I. INTRODUCTION

The possibility of increasing the performances of interferometers by using quantum light represents one of the most interesting uses of quantum states for overcoming classical limits of measurements. The first approach proposed with this aim was based on exploiting squeezed light for reducing the noise level in interferometers [1–4] and recently has found application in gravitational waves detectors [5–7]. Another approach considers the use of entanglement in phase estimation and in particular the possibility offered by the use of NOON states [8–11]. However, even if this approach generates significant conceptual interest and could find very interesting applications in the future, nowadays the difficulty in producing high-N entangled states and the fragility to noise and losses of these schemes strongly limits their real possible use.

In the realm of continuous-variable states, also two-mode squeezed light can be a resource for quantum interferometry when exploited in active interferometers [12,13]. Recently, correlation in photon number in a two-mode squeezed vacuum or twin-beam (TWB) state [14] has been demonstrated to be an important tool for beating shot noise [15,16] and for realizing a quantum protocol effectively robust against noise and losses [17]. These results prompted the study of the possibility of improving the so-called holometer by exploiting quantum light in the continuous-variable regime as squeezed light or TWBs [18,19]. The holometer is a setup based on two Michelson interferometers (MIs) and aimed at detecting the so-called holographic noise (HN): This is a basic form of noise conjectured in quantum gravity theories that would derive from a specific noncommutativity of the spatial degrees of freedom at the Planck scale [20]. This noise, albeit very small, should be correlated when the two MIs are parallel, so as to be in the respective light cones, and should be uncorrelated when one arm is rotated to be oriented in the opposite direction for the two MIs. The evident huge impact of the discovery of HN, the first evidence of quantum gravity [21–26], motivates an accurate analysis of the possibility of improving the holometer performance. In this paper we detail and complete the analysis of Ref. [18] identifying operative situations where the use of quantum light would allow one to greatly increase the performance of a double interferometer such as the holometer.

Specifically, in Ref. [18] we investigated an unusual but potentially powerful system consisting of two interferometers whose correlation of output ports signals is measured (see Fig. 1). This kind of double interferometric system can represent a breakthrough for detecting a faint correlated signal that would remain otherwise hidden even using the most sensitive individual classical interferometric devices, limited by the shot noise. In contrast, if the two interferometers experience identical fluctuations, this signal should emerge in a correlation measurement of their output, while the fluctuations due to shot noise and other independent contributions will vanish. The first experimental realization of this scheme using coherent beams (stabilized lasers), exactly for HN detection, is already being implemented at Fermilab [19]. Other applications can be envisaged such as for the generation of gravitational wave detectors.

In Ref. [18] we introduced a rigorous quantum model for describing the system. As opposed to the standard phase measurement in a single interferometer, which involves a first-order expectation value of the output, in the double interferometric scheme the quantity under estimation is the covariance of the two outputs, which is a second-order quantity, thus the associated uncertainty is a fourth-order function. Notwithstanding this difference, we demonstrated how the injection of quantum light at the input ports, which would remain unused in the classical holometer configuration, can boost the sensitivity of the device. In addition to the classical intense coherent beam, we considered the use of both an independent squeezed beam (SQB) and a correlated state

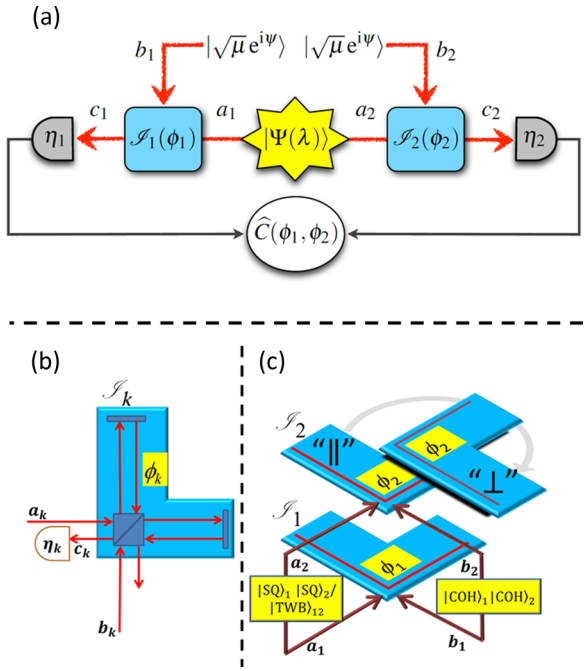

FIG. 1. (Color online) (a) Double-interferometer scheme. The modes of the bipartite input state $|\Psi(\lambda)\rangle$ are mixed with two identical coherent states $|\sqrt{\mu}e^{i\psi}\rangle$ in two interferometers $\mathscr{I}_1(\phi_1)$ and $\mathscr{I}_2(\phi_2)$. A joint detection is performed and the observable $\widehat{C}(\phi_1,\phi_2)$ is measured. (b) Scheme of the single Michelson interferometer $\mathscr{I}_k(\phi_k)$, where ϕ_k is the relative phase shift between the two arms. (c) The two measurement configurations of the holometer suggested in order to reveal the holographic noise. In the ∥ configuration the arms of the two interferometers are parallel and they share the same light cone, while in the ⊥ configuration one of the two interferometers is rotated by 90°. See the text for further details.

such as the TWB. The ideal experiment described theoretically in Ref. [18] is however extremely challenging for a practical experimental implementation. In particular, in order to provide optimal quantum enhancement, the central phases of the two interferometers must be set exactly at zero. As we will show in this paper, this is a critical issue since minimal deviations from this working regime completely compromise the advantages of the entangled strategy. Furthermore, the balanced readout configuration explored in the SQB case would require simultaneously a high dynamic range and fast and high-resolution detectors that are not yet available. Here we present a framework in which a more complete and general study of the double interferometric system is provided, leading also to the depiction of a more experiment-oriented configuration of the system in terms of readout strategy and parameters choice.

The paper is structured as follows. Section II presents the interferometric scheme considered throughout the paper. In Sec. III we analyze the correlation properties at the output ports of the interferometer in the TWB case, demonstrating that there are two relevant regimes with different behavior of the system according to the balance between the quantum and classical light at the interferometer dark ports. In Sec. IV we describe in detail a model establishing the connection between a generic measurement operator (observable) and the estimation of the phase covariance introduced by a correlated faint phase signal such as HN. Then we focus on two specific quantum strategies: the use of the TWB state and the measure of the photon number difference or the use of two independent squeezed states and the measure of quadrature covariance. In both cases we evaluate the lower bound to the uncertainty in the phase-covariance estimation given by photon noise as a function of the fundamental parameters: the interferometer's central phases, the quantum and classical beam intensities, and detection efficiency. The results of our investigation are reported in Sec. V. For rather challenging conditions, namely, almost ideal efficiency and perfect control of the stability of the interferometer's central phases, the TWB state could deliver an extraordinary advantage due to its photon number correlation at the quantum level (entanglement). This regime corresponds to the situation analyzed in [18]. Conversely, there exists a less demanding regime, in which quantum strategies provide good enhancement in a more favorable experimental condition. In this case, for both TWBs and SQBs the expression of the minimal uncertainty presents the usual scaling with losses and with the quantum light intensity, typical of a single-interferometer phase estimation using a strong local oscillator and squeezed light. We summarize in Sec. VI.

II. INTERFEROMETRIC SCHEME

Let us consider a system as depicted in Fig. 1(a). Two interferometers $\mathscr{I}_k$ $(k = 1,2)$ [see Fig. 1(b)] are injected at the ports denoted by the mode annihilation operator b_k by a couple of identical coherent beams $|\sqrt{\mu}e^{i\psi}\rangle_{b_k}$, while the remaining ports identified by the mode operator a_k (unused in the classical scheme) are fed with a quantum state $|\Psi(\lambda)\rangle_{a_1,a_2}$, where λ is the mean number of photons in each mode. The readout ports are denoted by the mode operator c_k, which will be a function of the phases shifts ϕ_k between the arms of each interferometer $c_k = c_k(\phi_k)$. Therefore, a final combination of the outputs results in an observable $\widehat{C}(c_1,c_2,\text{H.c.}) = \widehat{C}(\phi_1,\phi_2)$. A proper choice of the operator $\widehat{C}$ leads to an estimation of the phase-noise correlation. Here it is useful to recall the property that the input-output operator relations of a linear interferometer (for example, a Michelson-type) are equivalent to the ones of a beam splitter (BS) with a transmission coefficient $\tau = \cos^2(\phi/2)$. In the rest of the paper we will refer to τ as the interferometer transmission.

The losses in the system are taken into account by considering in both channels two identical detectors with the same quantum efficiency η. If only the classical field is injected, the photon counting statistics at the output ports is simply the one of coherent beams after the reflection probability $1-\tau_k$ and detection probability η,

$$\langle N_k\rangle^{\text{coh}}_{\eta\tau_k} = \langle \delta N_k^2\rangle^{\text{coh}}_{\eta\tau_k} = \eta\mu(1-\tau_k), \tag{1a}$$

$$\langle \delta N_1 \delta N_2\rangle^{\text{coh}}_{\eta\tau_1\tau_2} \equiv 0. \tag{1b}$$

In the following we consider two possible quantum states feeding the free input ports of $\mathscr{I}_k$ and two related readout strategies.

Readout strategy 1: The TWB state. The TWB correlated state can be expressed in the Fock bases $\{|m\rangle_{a_k}\}$ as

$$|\Psi(\lambda)\rangle_{a_1,a_2} = \frac{1}{\sqrt{1+\lambda}} \sum_{m=0}^{\infty} \left(e^{i\theta} \sqrt{\frac{\lambda}{1+\lambda}} \right)^m |m,m\rangle_{a_1,a_2}, \quad (2)$$

where $|m,m\rangle_{a_1,a_2} = |m\rangle_{a_1} \otimes |m\rangle_{a_2}$ and θ is the phase, which we set in the following to $\theta = 0$ without loss of generality. The TWB presents perfect correlations in the photon number $m_k \equiv a_k^\dagger a_k$, meaning that ${}_{a_1,a_2}\langle\Psi(\lambda)|(m_1 - m_2)^M|\Psi(\lambda)\rangle_{a_1,a_2} = 0$ for all integers $M > 0$. This implies, for example, that the variance of the photons number difference $\langle\delta(m_1 - m_2)^2\rangle$, where $\delta m \equiv m - \langle m\rangle$, is identically null. It also suggests that the measurement operator should be chosen in the same form $\widehat{C}(\phi_1,\phi_2) = \langle(N_1 - N_2)^M\rangle$, since this should correspond to a reduction of the photon noise in the measurement, finally improving the sensitivity.

By using the equivalence between interferometers and BSs mentioned before, we can calculate the photon statistics of TWBs transmitted to the output ports (in the absence of a classical coherent field) and detected with quantum efficiency η. The mean photon number, the variance, and the covariance are

$$\langle N_k\rangle_{\eta\tau_k}^{\mathrm{TWB}} = \eta\tau_k\lambda, \quad (3a)$$

$$\langle\delta N_k^2\rangle_{\eta\tau_k}^{\mathrm{TWB}} = \eta\tau_k\lambda(1 + \eta\tau_k\lambda), \quad (3b)$$

$$\langle\delta N_1\delta N_2\rangle_{\eta\tau_1\tau_2}^{\mathrm{TWB}} = \eta^2\tau_1\tau_2\lambda(1+\lambda), \quad (3c)$$

respectively.

Readout strategy 2: Two squeezed states. The state of two uncorrelated single-mode squeezed states is written

$$|\xi\rangle_{a_1} \otimes |\xi\rangle_{a_2} = S_{a_1}(\xi)S_{a_2}(\xi)|0\rangle_{a_1} \otimes |0\rangle_{a_2},$$

where $S_{a_k}(\xi) = \exp[\frac{1}{2}\xi(a_k^\dagger)^2 - \frac{1}{2}\xi^*(a_k)^2]$ is the squeezing operator. If we set $\xi = |\xi|e^{i\theta_\xi}$, then $\lambda = \sinh^2|\xi|$ represents the average number of photons of the squeezed vacuum, taken to be equal in both modes.

Defining the quadrature of the field as

$$x_k = \frac{a_k + a_k^\dagger}{\sqrt{2}}, \quad y_k = \frac{a_k - a_k^\dagger}{i\sqrt{2}}$$

and supposing that y_k is the squeezed quadrature and x_k the antisqueezed one, i.e., $\xi_k = |\xi_k| \geqslant 0$, it is known that in the single interferometer the injection of the squeezed field provides a fixed factor $\langle\delta y_k^2\rangle = e^{-2\xi_k}$ of resolution enhancement for arbitrary brightness of the coherent beam [1]. We expected that the increased resolution in the estimation of the phase shifts ϕ_1 and ϕ_2 separately reflects in a better estimation of their correlation if the correlation of the squeezed quadratures X_k of the output modes c_k are considered, namely, $\widehat{C} = X_1 X_2$.

III. CORRELATIONS AT THE READOUT PORTS

As a figure of merit for the correlations at the readout ports, we study the noise reduction parameter $\mathrm{NRF}_\pm \equiv \langle\delta(N_1 \pm N_2)^2\rangle/\langle N_1 + N_2\rangle$ [27–30], i.e., the ratio between the variance of the photon number sum (difference) and the corresponding shot-noise limit. In particular, if $\mathrm{NRF}_- < 1$, the bipartite state exhibits nonclassical correlations and its value also determines the quantum enhancement achievable in certain sensing [17] and imaging protocols [15]. Analogously, $\mathrm{NRF}_+ < 1$ can be interpreted as a strong signature of anticorrelation of the photon number beyond classical limits. The BS-like transformation allows evaluating the fluctuation of the fields at the output ports as a function of the input field. In particular, if we consider the TWBs as input, one gets

$$\langle N_k\rangle = \langle N\rangle_{\eta\tau_k}^{\mathrm{TWB}} + \langle N\rangle_{\eta\tau_k}^{\mathrm{coh}}, \quad (4a)$$

$$\langle\delta N_k^2\rangle = \langle\delta N^2\rangle_{\eta\tau_k}^{\mathrm{TWB}} + \langle\delta N^2\rangle_{\eta\tau_k}^{\mathrm{coh}} + 2\langle N\rangle_{\eta\tau_k}^{\mathrm{TWB}}\langle N\rangle_{\eta\tau_k}^{\mathrm{coh}}, \quad (4b)$$

$$\langle\delta N_1\delta N_2\rangle = \langle\delta N_1\delta N_2\rangle_{\eta\tau_1\tau_2}^{\mathrm{TWB}} - 2\sqrt{\langle\delta N_1\delta N_2\rangle_{\eta\tau_1\tau_2}^{\mathrm{TWB}}\langle N\rangle_{\eta\tau_1}^{\mathrm{coh}}\langle N\rangle_{\eta\tau_2}^{\mathrm{coh}}}\cos(2\psi) \quad (4c)$$

and the explicit expression, as a function of the parameters, can be directly obtained by substituting the quantities according to Eqs. (1) and (3). In particular Eq. (4c) shows that the covariance is composed of the TWB covariance $\langle\delta N_1\delta N_2\rangle_{\eta\tau_1\tau_2}^{\mathrm{TWB}}$ and a second term containing the phase of the coherent field ψ, originating from the BS interaction of the two fields. Interestingly, the choice of $\psi = \pi/2$ maximizes the covariance, while for $\psi = 0$ the covariance can even be negative (an anticorrelation of photon numbers).

The $\mathrm{NRF}_\pm$ can be easily calculated from Eqs. (4) by exploiting the identity $\langle\delta(N_1 \pm N_2)^2\rangle = \langle\delta N_1^2\rangle + \langle\delta N_2^2\rangle \pm 2\langle\delta N_1\delta N_2\rangle$. From now on, for the sake of simplicity, we assume the same interferometer transmission, namely, $\tau_1 = \tau_2 = \tau$, and thus $\langle N_k\rangle_{\eta\tau}^{\mathrm{TWB}} = \langle N\rangle_{\eta\tau}^{\mathrm{TWB}}$ and $\langle N_k\rangle_{\eta\tau}^{\mathrm{coh}} = \langle N\rangle_{\eta\tau}^{\mathrm{coh}}$, $k = 1,2$. We have

$$\mathrm{NRF}_\pm = 1 + \frac{(1/2)\langle\delta(N_1 \pm N_2)^2\rangle_{\eta\tau}^{\mathrm{TWB}} - \langle N\rangle_{\eta\tau}^{\mathrm{TWB}} + 2\langle N\rangle_{\eta\tau}^{\mathrm{coh}}\left[\langle N\rangle_{\eta\tau}^{\mathrm{TWB}} \mp \sqrt{\langle\delta N_1\delta N_2\rangle_{\eta\tau}^{\mathrm{TWB}}}\cos(2\psi)\right]}{\langle N\rangle_{\eta\tau}^{\mathrm{TWB}} + \langle N\rangle_{\eta\tau}^{\mathrm{coh}}}. \quad (5)$$

We note that NRF_- is minimized for $\psi = \pi/2$ (corresponding to the optimization of the photon number correlation), while NRF_+ is minimized when $\psi = 0$ (corresponding to the optimization of the anticorrelation): In the following we will always assume these two phase choices. The (minimized) NRF_- and NRF_+ are plotted in Figs. 2 and 3, respectively, for $\eta = 1$ and different values of the other parameters involved. In order to analyze the behavior of $\mathrm{NRF}_\pm$ and for the forthcoming discussion of the results concerning the phase-covariance estimation in Sec. V, it is useful to distinguish two regimes.

A. Regime A: TWB-like correlations

In this regime, which has been studied in Ref. [18], we have $\langle N\rangle_{\eta\tau}^{\mathrm{coh}} \ll \langle N\rangle_{\eta\tau}^{\mathrm{TWB}}$ or, equivalently, $\kappa \equiv \mu(1-\tau)/\tau\lambda \ll 1$: Here the intensity at the readout port is dominated by the TWBs

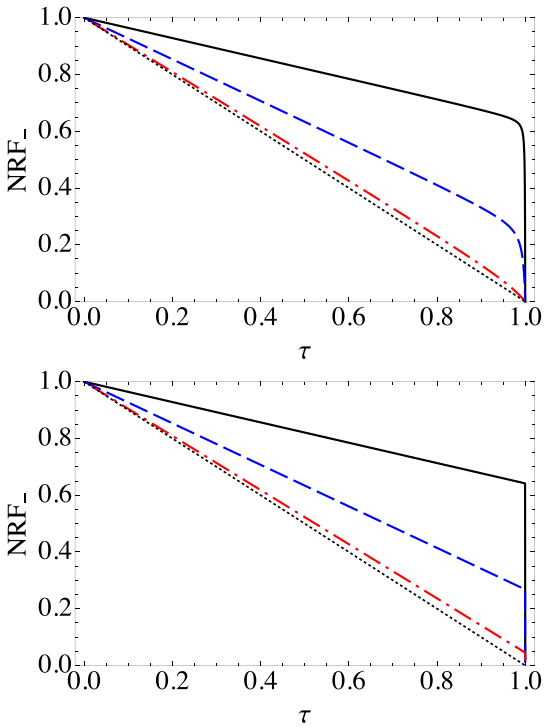

FIG. 2. (Color online) Plots of NRF_- given in Eq. (5) with $\psi = \pi/2$ and $\eta = 1$ versus the interferometer transmission τ. We set $\mu = 10^2$ (top) and $\mu = 10^5$ (bottom) and use different values of λ: $\lambda = 0.05$ (black solid line), 0.5 (blue dashed line), and 5.0 (red dot-dashed line). The dotted lines refer to the limit $\lambda \to \infty$. See the text for details.

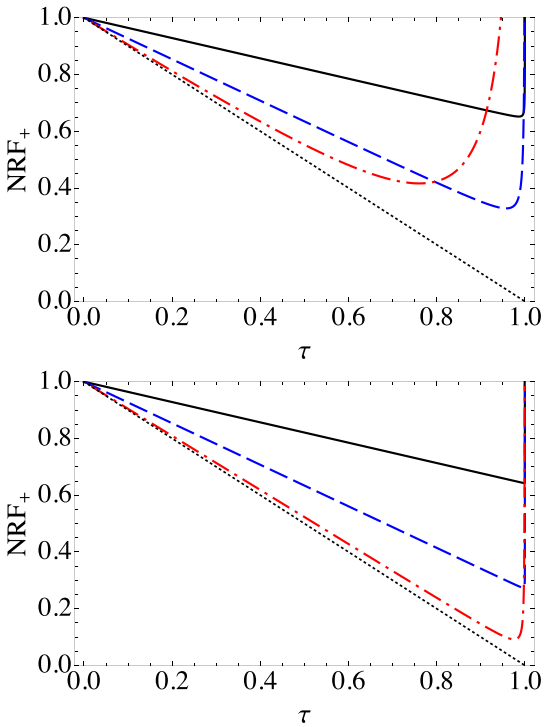

FIG. 3. (Color online) Plots of NRF_+ given in Eq. (5) with $\psi = 0$ and $\eta = 1$ versus the interferometer transmission τ. We set $\mu = 10^2$ (top) and $\mu = 10^5$ (bottom) and use different values of λ: $\lambda = 0.05$ (black solid line), 0.5 (blue dashed line), and 5.0 (red dot-dashed line). The dotted lines refer to the limit $\lambda \to \infty$. See the text for details.

and thus $\mathrm{NRF}_\pm \approx \langle \delta(N_1 \pm N_2)^2 \rangle_{\eta\tau}^{\mathrm{TWB}} / (2\langle N \rangle_{\eta\tau}^{\mathrm{TWB}})$ and, as it is evident in Figs. 2 and 3, NRF_- drastically decreases whereas NRF_+ grows accordingly. Of course, the condition $\langle N \rangle_{\eta\tau}^{\mathrm{coh}} \ll \langle N \rangle_{\eta\tau}^{\mathrm{TWB}}$ appears to be quite challenging to achieve in the relevant case of practical interest in which the coherent mode is largely populated: The larger μ is, the closer to unity the interferometer transmission τ of the interferometers has to be.

If we expand the noise reduction factors of Eq. (5) up to the first order in $1 - \tau$ we have (we use the minimization conditions on ψ)

$$\mathrm{NRF}_- \approx 1 - \eta + \eta(1-\tau)\left[1 + 2\mu + \frac{\mu(1 - 2\sqrt{\lambda^2+\lambda})}{\lambda}\right] \tag{6}$$

and

$$\mathrm{NRF}_+ \approx 1 + \eta(1+2\lambda) + \eta(\tau - 1)\left[1 + 2\lambda + \frac{\mu(1 - 2\sqrt{\lambda^2+\lambda})}{\lambda}\right], \tag{7}$$

respectively, recovering, in the limit $\lambda \gg 1$, the expression of the noise reduction factor for TWBs in the presence of losses [15], namely, $\mathrm{NRF}_- \approx 1 - \eta\tau$ and $\mathrm{NRF}_+ \approx 1 + \eta\tau(1 + 2\lambda)$. It is also worth noting that while $\mathrm{NRF}_- < 1$, we have $\mathrm{NRF}_+ > 1$ for $\tau > \tau_{\mathrm{th}}$, where

$$\tau_{\mathrm{th}} = 1 - \frac{\lambda(1+2\lambda)}{\lambda(1+2\lambda) + 2\mu(\sqrt{\lambda^2+\lambda} - \lambda)}. \tag{8}$$

In principle, this regime allows exploiting the perfect TWB-like correlation, with a large classical power circulating into the interferometer, thus obtaining surprising quantum enhancement in the phase correlation estimation, as we will further discuss below.

B. Regime B: Bright quantum correlation

When the coherent power reflected to the measuring port is much higher than the transmitted power of the TWBs, namely, $\langle N \rangle_{\eta\tau}^{\mathrm{coh}} \gg \langle N \rangle_{\eta\tau}^{\mathrm{TWB}}$ or $\mu(1-\tau) \gg \lambda\tau$, Eq. (5) reduces to

$$\mathrm{NRF}_\pm \simeq 1 + 2\langle N \rangle_{\eta\tau}^{\mathrm{TWB}} \pm 2\sqrt{\langle \delta N_1 \delta N_2 \rangle_{\eta\tau}^{\mathrm{TWB}}}\cos(2\psi).$$

Introducing the explicit expressions of the various moments of the photon number distribution, we have [we still use the condition of ψ minimizing the corresponding noise reduction factor, namely, $\mathrm{NRF}_- \equiv \mathrm{NRF}_-(\psi = \pi/2)$ and $\mathrm{NRF}_+ \equiv \mathrm{NRF}_+(\psi = 0)$]

$$\mathrm{NRF}_\pm \approx 1 - 2\eta\tau(\sqrt{\lambda^2+\lambda} - \lambda). \tag{9}$$

If $\lambda \gtrsim 3$ the last expansion is well approximated by $\mathrm{NRF}_\pm \approx 1 - \eta\tau + \eta\tau/4\lambda$, which, in the limit $\lambda \gg 1$, reduces to $\mathrm{NRF}_\pm \approx 1 - \eta\tau$ (see the dotted lines in Figs. 2 and 3). It is worth noting that in this regime and for the proper choice of the phase of the classical fields the $\mathrm{NRF}_\pm$ is always smaller than 1, whatever the intensity of TWB and losses. Thus, N_1 and N_2 are always correlated (or anticorrelated) beyond the classical

limit. It is possible to switch between quantum correlation and quantum anticorrelation just by acting on the phase ψ of the classical fields. Even more interesting, the correlation can be extremely bright, because the mean number of photon at the readout ports is determined by the brightness of the classical beam $\langle N\rangle_{\eta\tau}^{\rm coh}=\eta\mu(1-\tau)$, which can be extremely high in real experiments. It is clear from Eq. (9) that the highest correlation is obtained when $\lambda\gg 1$ and at the same time the interferometer transmission τ approaches 1. For example, for reasonable values of $\tau\approx 0.9$, $\mu\approx 10^{15}$, and $\lambda\approx 3$ we obtain $\mathrm{NRF}_{\pm}\approx 0.08$ [we are still in the present regime B since the mean intensity of the output signal is $(1-\tau)\mu\approx 10^{13}$ while $\tau\lambda\approx 2.97$].

IV. ESTIMATION OF PHASE CORRELATION DUE TO HOLOGRAPHIC NOISE

Since the phase fluctuations due to the HN are expected to be extremely small, we can expand $\widehat{C}(\phi_1,\phi_2)$ around the central values of the phase $\phi_{k,0}$ of the interferometer $\mathscr{I}_k$ $(k=1,2)$, namely,

$$\begin{aligned}\widehat{C}(\phi_1,\phi_2)\approx\ & \widehat{C}(\phi_{1,0},\phi_{2,0})+\Sigma_k\partial_{\phi_k}\widehat{C}(\phi_{1,0},\phi_{2,0})\delta\phi_k\\ &+\frac{1}{2}\Sigma_k\partial^2_{\phi_k,\phi_k}\widehat{C}(\phi_{1,0},\phi_{2,0})\delta\phi_k^2\\ &+\partial^2_{\phi_1,\phi_2}\widehat{C}(\phi_{1,0},\phi_{2,0})\delta\phi_1\delta\phi_2,\end{aligned}\tag{10}$$

where $\delta\phi_k=\phi_k-\phi_{k,0}$ and $\partial^{h+k}_{\phi_1^h,\phi_2^k}\widehat{C}(\phi_{1,0},\phi_{2,0})$ is the $(h+k)$th-order derivative of $\widehat{C}(\phi_1,\phi_2)$ calculated at $\phi_k=\phi_{k,0}$. In order to reveal the HN, the holometer exploits two different configurations [Fig. 1(c)]: the one $\parallel$ where HN correlates the interferometers and the other $\perp$ where the effect of HN vanishes. The statistical properties of the phase-shift (PS) fluctuations due to the HN may be described by the joint probability density functions $f_{\parallel}(\phi_1,\phi_2)$ and $f_{\perp}(\phi_1,\phi_2)$. We make two reasonable hypotheses about $f_x(\phi_1,\phi_2)$, $x=\parallel,\perp$. First, the marginals $\mathscr{F}_x^{(k)}(\phi_k)=\int d\phi_h f_x(\phi_k,\phi_h)$, $h,k=1,2$ with $k\neq h$, are exactly the same in the two configurations, i.e., $\mathscr{F}_{\parallel}^{(k)}(\phi_k)=\mathscr{F}_{\perp}^{(k)}(\phi_k)$: One cannot distinguish between the two configurations just by addressing one interferometer. Second, only in configuration $\perp$ it is $f_{\perp}(\phi_1,\phi_2)=\mathscr{F}_{\perp}^{(1)}(\phi_1)\mathscr{F}_{\perp}^{(2)}(\phi_2)$, i.e., there is no correlation between the PSs due to the HN [18]. Now the expectation of any operator $\widehat{O}(\phi_1,\phi_2)$ should be averaged over f_x, namely, $\langle\widehat{O}(\phi_1,\phi_2)\rangle\to\mathscr{E}_x[\widehat{O}(\phi_1,\phi_2)]\equiv\int\langle\widehat{O}(\phi_1,\phi_2)\rangle f_x(\phi_1,\phi_2)d\phi_1 d\phi_2$. In turn, by averaging the expectation of Eq. (10), we have

$$\begin{aligned}\mathscr{E}_x[\widehat{C}(\phi_1,\phi_2)]\approx\ & \langle\widehat{C}(\phi_{1,0},\phi_{2,0})\rangle\\ &+\frac{1}{2}\Sigma_i\langle\partial^2_{\phi_i,\phi_i}\widehat{C}(\phi_{1,0},\phi_{2,0})\rangle\mathscr{E}_x[\delta\phi_i^2]\\ &+\langle\partial^2_{\phi_1,\phi_2}\widehat{C}(\phi_{1,0},\phi_{2,0})\rangle\mathscr{E}_x[\delta\phi_1\delta\phi_2],\end{aligned}\tag{11}$$

where we used $\mathscr{E}_x[\delta\phi_k]=0$. Then, according to the assumptions on $f_x(\phi_1,\phi_2)$, we have $\mathscr{E}_{\parallel}[\delta\phi_k^2]=\mathscr{E}_{\perp}[\delta\phi_k^2]$ and $\mathscr{E}_{\perp}[\delta\phi_1\delta\phi_2]=\mathscr{E}_{\perp}[\delta\phi_1]\mathscr{E}_{\perp}[\delta\phi_2]=0$ and from Eq. (11) it follows that the phase-covariance may be written as

$$\mathscr{E}_{\parallel}[\delta\phi_1\delta\phi_2]\approx\frac{\mathscr{E}_{\parallel}[\widehat{C}(\phi_1,\phi_2)]-\mathscr{E}_{\perp}[\widehat{C}(\phi_1,\phi_2)]}{\langle\partial^2_{\phi_1,\phi_2}\widehat{C}(\phi_{1,0},\phi_{2,0})\rangle},\tag{12}$$

which is proportional to the difference between the mean values of the operator $\widehat{C}(\phi_1,\phi_2)$ as measured in the two configurations $\parallel$ and $\perp$.

Now one has to reduce as much as possible the uncertainty associated with its measurement, namely (we still assume $\delta\phi_1,\delta\phi_2\ll 1$),

$$\mathscr{U}(\delta\phi_1\delta\phi_2)\approx\frac{\sqrt{\mathrm{Var}_{\parallel}[\widehat{C}(\phi_1,\phi_2)]+\mathrm{Var}_{\perp}[\widehat{C}(\phi_1,\phi_2)]}}{\left|\langle\partial^2_{\phi_1,\phi_2}\widehat{C}(\phi_{1,0},\phi_{2,0})\rangle\right|},\tag{13}$$

where $\mathrm{Var}_x[\widehat{C}(\phi_1,\phi_2)]\equiv\mathscr{E}_x[\widehat{C}^2(\phi_1,\phi_2)]-\mathscr{E}_x[\widehat{C}(\phi_1,\phi_2)]^2$. Under the same hypotheses used for deriving Eq. (12) we can calculate the variance of $\widehat{C}(\phi_1,\phi_2)$ as

$$\begin{aligned}\mathrm{Var}_x[\widehat{C}(\phi_1,\phi_2)]\approx\ & \mathrm{Var}[\widehat{C}(\phi_{1,0},\phi_{2,0})]+\Sigma_k A_{kk}\mathscr{E}_x\left[\delta\phi_k^2\right]\\ &+A_{12}\mathscr{E}_x[\delta\phi_1\delta\phi_2],\end{aligned}\tag{14}$$

where

$$\begin{aligned}A_{kk}=\ & \langle\widehat{C}(\phi_{1,0},\phi_{2,0})\partial^2_{\phi_k,\phi_k}\widehat{C}(\phi_{1,0},\phi_{2,0})\rangle+\langle\left[\partial_{\phi_k}\widehat{C}(\phi_{1,0},\phi_{2,0})\right]^2\rangle\\ &-\langle\widehat{C}(\phi_{1,0},\phi_{2,0})\rangle\langle\partial^2_{\phi_k,\phi_k}\widehat{C}(\phi_{1,0},\phi_{2,0})\rangle\end{aligned}\tag{15}$$

$$\begin{aligned}A_{12}=\ & 2\langle\widehat{C}(\phi_{1,0},\phi_{2,0})\partial^2_{\phi_1,\phi_2}\widehat{C}(\phi_{1,0},\phi_{2,0})\rangle\\ &+2\langle\partial_{\phi_1}\widehat{C}(\phi_{1,0},\phi_{2,0})\partial_{\phi_2}\widehat{C}(\phi_{1,0},\phi_{2,0})\rangle\\ &-\langle\widehat{C}(\phi_{1,0},\phi_{2,0})\rangle\langle\partial^2_{\phi_1,\phi_2}\widehat{C}(\phi_{1,0},\phi_{2,0})\rangle.\end{aligned}\tag{16}$$

Analyzing Eq. (14), we note the presence of a zeroth-order contribution that does not depend on the PS's intrinsic fluctuations and represents the quantum photon noise of the measurement described by the operator $\widehat{C}(\phi_1,\phi_2)$ evaluated on the optical quantum states sent into the holometer. The statistical characteristics of the phase noise enter as second-order contributions in Eq. (14) from each interferometer plus a contribution coming from phase correlation between them.

In this paper we specifically focus on the problem of reducing the photon noise below the shot noise in the measurement of the HN; therefore, in the following we will assume the zeroth-order contribution being the dominant one. Of course, this means that one should look for the HN in a region of the noise spectrum that is shot-noise limited. Since the HN is expected up to frequencies of tens of MHz, it follows that all the sources of mechanical vibration noise are suppressed. Therefore, the zeroth-order uncertainty that we will study here is

$$\mathscr{U}^{(0)}=\frac{\sqrt{2\,\mathrm{Var}[\widehat{C}(\phi_{1,0},\phi_{2,0})]}}{\left|\langle\partial^2_{\phi_1,\phi_2}\widehat{C}(\phi_{1,0},\phi_{2,0})\rangle\right|}.\tag{17}$$

A. TWB states

As we argued in Sec. II, when the TWB state is injected it should be promising to define the observable operator in the form $\widehat{C}(\phi_1,\phi_2)=(N_1-N_2)^M$, $M>0$, because of the perfect photon number correlation of the TWB state. In Sec. III we showed that at least up to the second order $M=2$, the strong nonclassical correlations are preserved at the output ports of the interferometers (for $\psi=\pi/2$), justifying the conjecture that an advantage in terms of noise reduction would be obtained if we can estimate the phase covariance starting

from the measurement of an observable of that form. We notice immediately that for $M = 1$, corresponding to the photon numbers difference, the proportional coefficient in Eq. (12), containing the double derivative with respect to both the phases, will be null. Thus, we have to move to the second-order measurement, i.e., $\widehat{C}(\phi_1,\phi_2) = [N_1(\phi_1) - N_2(\phi_2)]^2 = N_1^2 + N_2^2 - 2N_1N_2$. Hereinafter we also consider the same central phase of the two interferometers $\phi_{1,0} = \phi_{2,0} = \phi_0$.

According to Eq. (12) we get

$$\mathscr{E}_{\parallel}[\delta\phi_1\delta\phi_2] \approx \frac{\mathscr{E}_{\parallel}[N_1N_2] - \mathscr{E}_{\perp}[N_1N_2]}{\left\langle \partial^2_{\phi_1,\phi_2} N_1(\phi_0)N_2(\phi_0)\right\rangle}, \tag{18}$$

where we have used again the symmetry of the statistical properties of the two interferometers, in particular $\mathscr{E}_{\parallel(\perp)}[N_1^2] = \mathscr{E}_{\perp(\parallel)}[N_2^2]$. The covariance of the phase noise is proportional to the difference between the photon number correlation when the phase noise is correlated ($\parallel$) and when it is not ($\perp$), as one could expect. The uncertainty of the measurement, due to photon noise, can be obtained by Eq. (17), where $\mathrm{Var}[\widehat{C}(\phi_{1,0},\phi_{2,0})] = \langle[N_1(\phi_0) - N_2(\phi_0)]^4\rangle - \langle[N_1(\phi_0) - N_2(\phi_0)]^2\rangle^2$.

B. Independent squeezed states

It is rather intuitive that the most simple form of the measurement operator $\widehat{C}(\phi_1,\phi_2)$, which combines the squeezed quadratures measured at the readout port and has a non-null mixed derivative with respect to the phases $\partial^2_{\phi_1,\phi_2}\widehat{C} \neq 0$, would be the product Y_1Y_2 (where Y_k are the squeezed quadratures). However, to avoid the presence of a dc component in the measurement it turns out more useful to consider the fluctuation of the quadratures around their central value, therefore defining $\widehat{C} = \{Y_1(\phi_1) - \mathscr{E}[Y_1]\}\{Y_2(\phi_2) - \mathscr{E}[Y_2]\}$, where we have taken into account that $\mathscr{E}_{\parallel}[Y_k] = \mathscr{E}_{\perp}[Y_k] = \mathscr{E}[Y_k]$. The covariance of the phases is estimated according to Eq. (12) as

$$\mathscr{E}_{\parallel}[\delta\phi_1\delta\phi_2] \approx \frac{\mathscr{E}_{\parallel}[Y_1Y_2] - \mathscr{E}_{\perp}[Y_1Y_2]}{\left\langle \partial^2_{\phi_1,\phi_2} Y_1(\phi_0)Y_2(\phi_0)\right\rangle}. \tag{19}$$

Since the fluctuations of the quadratures due to quantum noise are independent in the two interferometers, the zeroth-order uncertainty on the measured observable remains $\mathrm{Var}[\widehat{C}(\phi_{1,0},\phi_{2,0})] = \langle\{Y_1(\phi_0) - \mathscr{E}[Y_1]\}^2\rangle\langle\{Y_2(\phi_0) - \mathscr{E}[Y_2]\}^2\rangle$ [see Eq. (17)].

V. RESULTS

The calculation of the variance of the measurement operator $\widehat{C}(\phi_0)$, in particular for the TWB case, involves many fourth-order terms of the photon number operator, i.e., the eighth-order product of field operator c_k and $c_k^\dagger$, and the calculation and the complete expression of this variance are too cumbersome to be reported here. Thus, we will present numerical results for the most significative regions inside the parameter space and we give some general expressions in particular relevant limits. First of all we need to define the classical benchmark to compare performance using quantum light. The uncertainty achievable in the estimation of the phase covariance, if only the coherent beams are used, is $\mathscr{U}_{\mathrm{cl}}^{(0)} = \sqrt{2}/\eta\mu\cos^2(\phi_0/2)$. It is worth noting that it scales as the detected number of photons, i.e., the *square* of the shot-noise limit typical of the single phase estimation. This

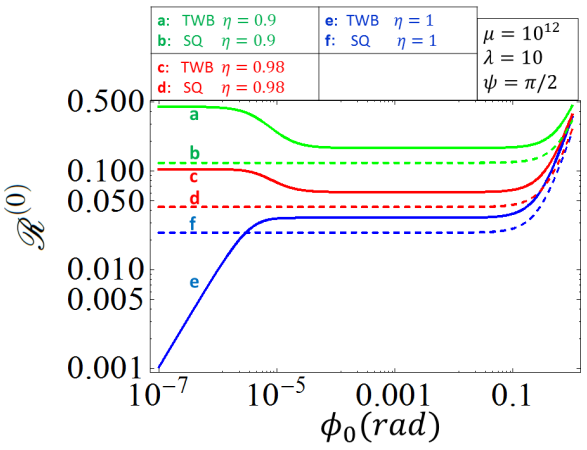

FIG. 4. (Color online) A log-log-plot of the quantum enhancements $\mathscr{R}^{(0)}_{\mathrm{TWB}}$ (solid lines) and $\mathscr{R}^{(0)}_{\mathrm{sq}}$ (dashed lines) as a function of the central phase ϕ_0 for three different values of η. When $\mathscr{R}^{(0)} < 1$ we have an advantage over the classical case. We set $\lambda = 10$, $\mu = 3 \times 10^{12}$, and $\psi = \pi/2$.

directly follows from the measurement of a second-order quantity, namely, the covariance of the phases [18]. As usual, it is clear that without any particular energy constraint, in order to reach high sensitivity in a phase-correlation measurement it is necessary to push the intensity of the classical field. Therefore, even the quantum strategy should face and improve the sensitivity when high power is circulating into the interferometers. Therefore, we will consider the limit $\mu \gg 1$.

Concerning the use of the two independent squeezed states, we can summarize the results in the following two equations for the ratio $\mathscr{R}^{(0)}_{\mathrm{sq}} = \mathscr{U}^{(0)}_{\mathrm{sq}}/\mathscr{U}^{(0)}_{\mathrm{cl}}$ in the limit $\mu \gg 1$:

$$\mathscr{R}^{(0)}_{\mathrm{sq}} \approx 1 - \frac{\eta(1+\cos\phi_0)}{2} + \frac{\eta\cos^2(\phi_0/2)}{4\lambda} \quad (\lambda \gg 1), \tag{20a}$$

$$\mathscr{R}^{(0)}_{\mathrm{sq}} \approx 1 - \eta(1+\cos\phi_0)\sqrt{\lambda}(1-\sqrt{\lambda}) \quad (\lambda \ll 1). \tag{20b}$$

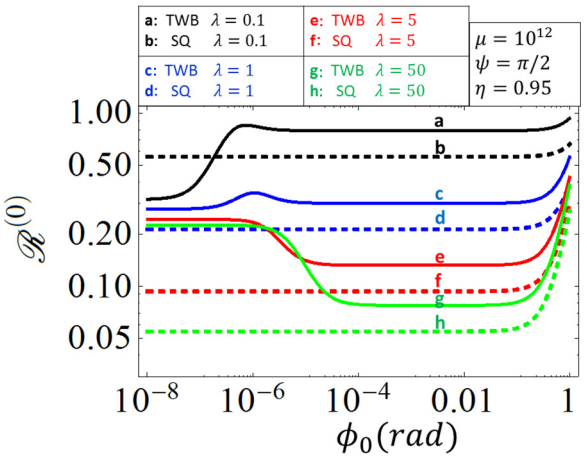

FIG. 5. (Color online) A log-log-plot of the quantum enhancements $\mathscr{R}^{(0)}_{\mathrm{TWB}}$ (solid lines) and $\mathscr{R}^{(0)}_{\mathrm{sq}}$ (dashed lines) as a function of the central phase ϕ_0 for four different values of the mean number of photons per mode λ of the quantum light. When $\mathscr{R}^{(0)} < 1$ we have an advantage over the classical case. We set $\eta = 0.95$, $\mu = 3 \times 10^{12}$, and $\psi = \pi/2$.

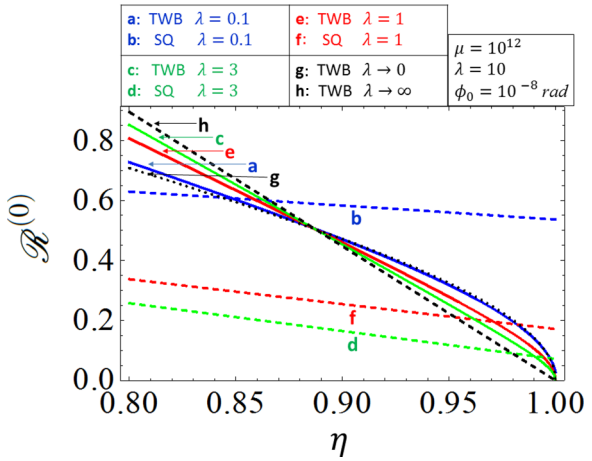

FIG. 6. (Color online) Plot of the quantum enhancements $\mathscr{R}^{(0)}_{\rm TWB}$ (solid lines) and $\mathscr{R}^{(0)}_{\rm sq}$ (dashed lines) as a function of the quantum efficiency η for several values of the mean number of photons per mode λ of the quantum light. When $\mathscr{R}^{(0)} < 1$ we have an advantage over the classical case. We set $\phi_0 = 10^{-8}$ rad, $\mu = 3 \times 10^{12}$, and $\psi = \pi/2$. We also report the limits for $\lambda \ll 1$ (line labeled g) and $\lambda \gg 1$ (line labeled h) referring to the TWB.

As a matter of fact, we expect that the advantages of using squeezing, and in general quantum light, is effective in the presence of a low loss level. Thus the most interesting regime is when the two interferometers transmit almost all the quantum light to the readout port. In this case the central phase must be close to 0, according to the BS-like behavior $\tau = \cos^2(\phi_0/2) \simeq 1$. In this limit Eqs. (20) reduce to $\mathscr{R}^{(0)}_{\rm sq} \approx 1 - \eta + \eta/4\lambda$ for $\lambda \gg 1$ and $\mathscr{R}^{(0)}_{\rm sq} \approx 1 - 2\eta\sqrt{\lambda}(1 - \sqrt{\lambda})$ for $\lambda \ll 1$. We can appreciate visually what it means by looking at Fig. 4. A flat region (on a logarithmic scale) appears in the uncertainty reduction as a function of the central phase ϕ_0 with the value given by $1 - \eta + \eta/4\lambda$. In the opposite limit of $\lambda \ll 1$ the advantage of squeezing is lost, according to Eq. (20b). For example, for $\lambda = 0.1$, represented in Fig. 5, the improvement is only 0.6.

Concerning the TWB state, one can clearly discern two different regions in both Figs. 4 and 5: one for really small values of the central phase, namely, $\phi_0 < 10^{-6}$, and the other in the range $10^{-5} < \phi_0 < 10^{-1}$. They correspond, for a specific

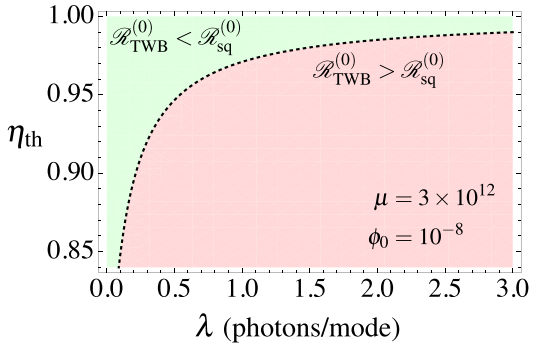

FIG. 7. (Color online) Plot of the threshold $\eta_{\rm th}$ (dashed line) as a function of λ for $\phi_0 = 10^{-8}$, $\mu = 3 \times 10^{12}$, and $\psi = \pi/2$. When $\eta > \eta_{\rm th}$ one has $\mathscr{R}^{(0)}_{\rm TWB} < \mathscr{R}^{(0)}_{\rm sq}$ (green region); otherwise $\mathscr{R}^{(0)}_{\rm TWB} \geq \mathscr{R}^{(0)}_{\rm sq}$ (red region).

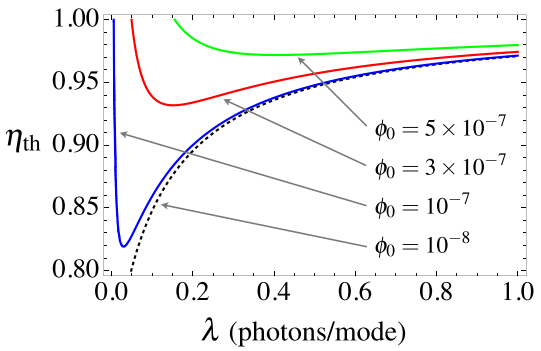

FIG. 8. (Color online) Plot of the threshold $\eta_{\rm th}$ as a function of λ for $\mu = 3 \times 10^{12}$, $\psi = \pi/2$, and different values of ϕ_0. When $\eta > \eta_{\rm th}$ one has $\mathscr{R}^{(0)}_{\rm TWB} < \mathscr{R}^{(0)}_{\rm sq}$; otherwise $\mathscr{R}^{(0)}_{\rm TWB} \geq \mathscr{R}^{(0)}_{\rm sq}$.

choice of the parameters indicated in the figures, to the two relevant regimes that have been individuated in Sec. III.

In the limit $\langle N\rangle^{\rm coh}_{\eta\tau} \ll \langle N\rangle^{\rm TWB}_{\eta\tau}$ we have the TWB-like correlations of regime A (see Sec. III). The condition is guaranteed if the central phases are close enough to zero, namely, $\phi_{1,0} = \phi_{2,0} \simeq 0$, meaning that the interferometer transmissivity approaches unity. This is the regime studied and reported in Ref. [18]. For an intense coherent beam and intense TWB source, i.e., $\mu \gg \lambda \gg 1$, one gets $\mathscr{R}^{(0)}_{\rm TWB} = \mathscr{U}^{(0)}_{\rm TWB}/\mathscr{U}^{(0)}_{\rm cl} \approx 2\sqrt{5}(1 - \eta)$, while in the case of faint TWBs $\lambda \ll 1$ and $\mu \gg 1$, the result is $\mathscr{R}^{(0)}_{\rm TWB} \approx \sqrt{2(1 - \eta)/\eta}$. In both cases the TWB state allows reaching a dramatic uncertainty reduction that approaches zero for $\eta \to 1$. This behavior is clearly shown in Fig. 6: The choice of μ and ϕ_0 ensures being in the TWB-like regime (at least for the considered range of values of λ). The ratio $\mathscr{R}^{(0)}_{\rm TWB}$ always drop to zero as $\eta \to 1$, whereas for η larger than a threshold value $\eta_{\rm th}$ we have $\mathscr{R}^{(0)}_{\rm TWB} < \mathscr{R}^{(0)}_{\rm sq}$ (see Figs. 7 and 8). In Fig. 6 we also reported the limits for $\lambda \ll 1$ (line g) and for $\lambda \gg 1$ (line h), respectively, in the presence of a TWB. Overall, we observe that for the quantum light intensity $\lambda > 1$ reachable in experiments nowadays (for example, $\lambda = 3$ in the picture) squeezing performs far better than TWBs except for highly demanding overall detection efficiency.

When $\langle N\rangle^{\rm coh}_{\eta\tau} \gg \langle N\rangle^{\rm TWB}_{\eta\tau}$ we find the right quantum correlations of regime B (see Sec. III), which correspond to the flat region shown in Figs. 4 and 5 for intermediate values of the central phase ϕ_0. Aside a constant factor, the uncertainty reduction for $\mu \gg 1$ behaves as for the two independent squeezing cases, specifically $\mathscr{R}^{(0)}_{\rm TWB} = \sqrt{2}\,\mathscr{R}^{(0)}_{\rm sq}$. It can be easily appreciated when comparing the corresponding curves for $\mathscr{R}^{(0)}_{\rm TWB}$ and $\mathscr{R}^{(0)}_{\rm sq}$ in the figures (note the logarithmic scale).

For the sake of completeness, we did the same analysis by considering the exploitation of the anticorrelations, defining the observable as $\widehat{C}(\phi_1,\phi_2) = (N_1 + N_2)^2 = N_1^2 + N_2^2 + 2N_1N_2$ (for $\psi = 0$) instead of the correlation when TWBs are injected, obtaining analogous results in the regime of $\mu(1 - \tau) \gg \lambda\tau$.

VI. CONCLUSION

In Sec. V we observed interesting features, leading to promising experimental conditions. Referring to Figs. 4 and 5,

there is an extended range of value of the central working phase ϕ_0 of the interferometers in which the uncertainty reduction achievable by adopting quantum light is stable, at the value $\mathscr{R}^{(0)} \approx 1 - \eta + \eta/4\lambda$, both with SQB and TWB states (apart from a factor $\sqrt{2}$ in the latter case). This kind of scaling is a well-known result of phase estimation in a single interferometer combining a coherent strong field and single-mode squeezed light (in fact $4\lambda \approx e^{2|\xi|}$ in the limit $4\lambda \gg 1$) [1]. Therefore, it turns out that a measurement of the phase correlation retains the same advantage of the single phase estimation. As an example, for $\eta = 0.9$ and $\lambda = 3$, which is compatible with the actual technology, we have an uncertainty reduction of 5.7 times in the single measurement. Since in any experiments $\mathscr{N}$ measurements are performed and the final uncertainty is $\mathscr{U}/\sqrt{\mathscr{N}}$, one would easily obtain the same sensitivity with a number of runs 30 times smaller, hence reducing the total measurement time of the same amount.

In contrast, only for the TWB state there exists a special setting of the central phase of the interferometer, when the classical field component is made negligible at the readout ports with respect to the TWB component. In this case, at least in principle, the uncertainty reaches the zero point, whatever the intensity of the TWBs. In particular, for faint TWBs ($\lambda \ll 1$) the uncertainty scales as $\mathscr{R}^{(0)}_{\mathrm{TWB}} \approx \sqrt{2(1-\eta)/\eta}$, while for intense TWBs ($\lambda \gg 1$) one gets $\mathscr{R}^{(0)}_{\mathrm{TWB}} \approx 2\sqrt{5}(1-\eta)$. Though at a first glance this effect looks rather exciting, Fig. 6 shows that in terms of absolute sensitivity the squeezing performance can be overtaken only for rather high detection efficiency. For example, for $\lambda = 3$ we expect $\mathscr{R}^{(0)}_{\mathrm{TWB}} < \mathscr{R}^{(0)}_{\mathrm{sq}}$ for $\eta \geqslant 0.99$. However, for limited quantum resources, namely, $\lambda < 1$, the TWB state performs better than squeezing already for smaller and more realistic efficiency values.

In conclusion, we have analyzed in detail a system of two interferometers aimed at the detection of extremely faint phase fluctuations. The idea behind this is that a correlated phase signal like the one introduced by the holographic noise could emerge by correlating the output ports of the interferometers, even when in the single interferometer it is confounded with the background. We demonstrated that injecting quantum light in the free ports of the interferometers can reduce the photon noise of the system beyond the shot noise, enhancing the resolution in the phase-correlation estimation. Our results confirm the benefit of using squeezed beams together with strong coherent beams in interferometry, even in this correlated case. On the other hand, our results concerning the possible use of TWBs pave the way to interesting and probably unexplored areas of application of bipartite entanglement and in particular the possibility of reaching a surprising uncertainty reduction exploiting new interferometric configurations, as in the case of the holometer.

ACKNOWLEDGMENTS

This work was supported by the EU through BRISQ2 (EU FP7 under Grant No. 308803) and QuProCS (Grant No. 641277). This work was made possible through the support of the John Templeton Foundation (Grant No. 48153).

[1] C. M. Caves, Phys. Rev. D **23**, 1693 (1981).
[2] M. G. A. Paris, Phys. Lett. A **201**, 132 (1995).
[3] S. Olivares and M. G. A. Paris, Opt. Spectrosc. **103**, 231 (2007).
[4] L. Pezzé and A. Smerzi, Phys. Rev. Lett. **100**, 073601 (2008).
[5] K. McKenzie, D. A. Shaddock, D. E. McClelland, B. C. Buchler, and P. K. Lam, Phys. Rev. Lett. **88**, 231102 (2002).
[6] J. Abadie *et al.*, Nat. Phys. **7**, 962 (2011).
[7] R. Demkowicz-Dobrzanski, K. Banaszek, and R. Schnabel, Phys. Rev. A **88**, 041802(R) (2013).
[8] S. F. Huelga, C. Macchiavello, T. Pellizzari, A. K. Ekert, M. B. Plenio, and J. I. Cirac, Phys. Rev. Lett. **79**, 3865 (1997).
[9] V. Giovannetti, S. Lloyd, and L. Maccone, Science **306**, 1330 (2004).
[10] A. N. Boto, P. Kok, D. S. Abrams, S. L. Braunstein, C. P. Williams, and J. P. Dowling, Phys. Rev. Lett. **85**, 2733 (2000).
[11] L. Pezzé, and A. Smerzi, in *Atom Interferometry*, Proceedings of the International School of Physics "Enrico Fermi," Course CLXXXVIII, Varenna, 2014, edited by G. M. Tino and M. A. Kasevich (IOS, Amsterdam, 2014), p. 691.
[12] W. N. Plick, J. P. Dowling, and G. S. Agarwal, New J. Phys. **12**, 083014 (2010).
[13] C. Sparaciari, S. Olivares, and M. G. A. Paris, J. Opt. Soc. Am. B **32**, 1354 (2015).
[14] M. V. Chekhova, G. Leuchs, and M. Zukowski, Opt. Commun. **337**, 27 (2015).
[15] G. Brida, L. Caspani, A. Gatti, M. Genovese, A. Meda, and I. Ruo Berchera, Phys. Rev. Lett. **102**, 213602 (2009).
[16] G. Brida, M. Genovese, and I. Ruo Berchera, Nat. Photon. **4**, 227 (2010).
[17] E. D. Lopaeva, I. Ruo Berchera, I. P. Degiovanni, S. Olivares, G. Brida, and M. Genovese, Phys. Rev. Lett. **110**, 153603 (2013).
[18] I. Ruo Berchera, I. P. Degiovanni, S. Olivares, and M. Genovese, Phys. Rev. Lett. **110**, 213601 (2013).
[19] https://holometer.fnal.gov/
[20] G. Hogan, Phys. Rev. D **85**, 064007 (2012).
[21] G. Amelino-Camelia, J. Ellis, N. E. Mavromatos, D. V. Nanopoulos, and S. Sarkar, Nature (London) **393**, 763 (1998).
[22] G. Amelino-Camelia, Nature (London) **398**, 216 (1999).
[23] G. Amelino-Camelia, Nature (London) **478**, 466 (2011).
[24] I. Pikovski, M. R. Vanner, M. Aspelmeyer, M. S. Kim, and Časlav Brukner, Nat. Phys. **8**, 393 (2012).
[25] J. D. Bekenstein, Phys. Rev. D **86**, 124040 (2012).
[26] P. Aschieri and L. Castellani, J. Geom. Phys. **60**, 375 (2010).
[27] M. Bondani, A. Allevi, G. Zambra, M. G. A. Paris, and A. Andreoni, Phys. Rev. A **76**, 013833 (2007).
[28] M. Lamperti, A. Allevi, M. Bondani, R. Machulka, V. Michálek, O. Haderka, and J. Peřina, J. Opt. Soc. Am. B **31**, 20 (2014).
[29] T. Iskhakov, M. V. Chekhova, and G. Leuchs, Phys. Rev. Lett. **102**, 183602 (2009).
[30] J. L. Blanchet, F. Devaux, L. Furfaro, and E. Lantz, Phys. Rev. Lett. **101**, 233604 (2008).